# The Effect of Used Fillers on the Strength Characteristics of Polymer Concrete Test Bodies

Jozef Zajac [1], Darina Dupláková [1], Michal Hatala [1], Dávid Goldyniak [1], Róbert Poklemba [1], Peter Šoltés [2]

[1]*Technical University of Košice, Faculty of Manufacturing Technologies with a seat in Prešov, Bayerova 1, 080 01 Prešov, Slovak Republic*
[2] *Ipm Solutions, s.r.o., Kamenná 11, 080 01 Prešov, Slovak Republic*

***Abstract*** **– This paper focuses on the effect of used fillers on the strength characteristics of polymer concrete test bodies. The first chapter contains a brief summary of the theoretical knowledge from the given issue. The second chapter contains the materials, machines, tools and equipment used in the manufacturing polymer concrete test bodies. The third chapter describes the production of polymer concrete castings and contains precise ratios of materials in individual test bodies. The fourth chapter describes the destructive testing of test bodies and interprets the measured results. Chapter Five summarizes the findings learned.**

***Keywords*** **– polymer concrete, destructive testing, compression strength, flexural strength, test bodies.**

## 1. Introduction

The supporting parts of lathes, milling machines, drills and other machine tools need to be improved on the construction and material side to handle the increasing dynamic and performance parameters of these machines. [1][2]Conventional materials, i.e. steel and cast iron have their limits, therefore it is appreciably important to consider replacing them with a suitable composite whose properties are within our influence by using proper composition. One solution is to use polymer concrete. [3][9]
Polymer concrete is essentially a composite material. These materials are characterized by a synergistic effect. [4][5] This means that the value of properties regarding resulting composite material is higher than the sum of the properties for each component separately. [10][11]

*Figure 1. Polymer concrete castings [6]*

Polymer concrete is composed of filler, binder and additives. The largest proportion in the mixture has a filler. The filler is the main carrier of the resulting properties. The fillers are divided into organic (andesite, basalt, dolomite, limestone, silica, etc.) and inorganic (glass, polymer, carbon, steel fibers, etc.). [7][8] The binder consists of resin and hardener. Epoxy resins are mostly used for the lowest volume shrinkage, good strength characteristics and chemical resistance. [12][13]

## 2. Materials, machines, tools and equipment

The following materials were used in manufacture the test bodies:

- fillers
  - **silica sand** – grain size 0,3 – 1 mm,
  - **Danube gravel** – grain size 4 – 8 mm,
  - **Danube gravel** – grain size 8 – 16 mm,

DOI: 10.18421/TEM83-14
https://dx.doi.org/10.18421/TEM83-14

**Corresponding author:** Darina Dupláková,
*Technical University of Košice, Faculty of Manufacturing Technologies with a seat in Prešov, Slovak Republic*
**Email:** *darina.duplakova@tuke.sk*

*Received: 06 March 2019.*
*Revised: 03 July 2019.*
*Accepted: 26 July 2019.*
*Published: 28 August 2019.*

- **dolomic limestone** – grain size 4 – 8 mm,
- **dolomic limestone** – grain size 8 – 16 mm,
- **andesite** – grain size 4 – 8 mm,
- **andesite** – grain size 8 – 16 mm,

- binder
  - **epoxy resin LH 160** – producer Havel-composites, Czech Republic. Universal epoxy resin. Excellent strength characteristics, low viscosity,
  - **hardener H 287** – producer Havel-composites, Czech Republic. Hardener providing long pot life of the mixture.

*Table 1. Properties of epoxy resin LH 160*

| | | |
|---|---|---|
| Viscosity at 25°C | mPa.s | 700 - 900 |
| Epoxy index | $mol.kg^{-1}$ | 0,55 – 0,60 |
| Epoxide mass equivalent | $g.mol^{-1}$ | 166 – 182 |
| Color | Gardner | max 3 |

*Table 2. Properties of hardener H 287*

| | | |
|---|---|---|
| Viscosity at 23°C | mPa.s | 80 – 100 |
| Density at 23°C | $g.cm^{-3}$ | 0,93 – 0,96 |
| Amine number | $mgKOH.g^{-1}$ | 450 – 500 |
| Color | Gardner | transparent blue |

The following machines were used in the manufacture of test bodies:

- vibration table **Lievers LTT 40/40.**


*Figure 2. Lievers LTT 40/40*

- electric stirrer **Makita UT1200.**

*Figure 3. Makita UT1200*

- plastic molds (brand: MATEST), in the shape of a cube with dimensions 150x150x150 mm and in the shape of joist with dimensions 100x100x500 mm according to STN EN 12390-1.

*Figure 4. Plastic molds*

- other equipment: trowel, plastic and glass containers, vaseline, personal protective equipment - glasses, gloves, respirator.

## 3. Manufacturing the test bodies

Manufacturing the polymer concrete test bodies was carried out at the Faculty of Manufacturing Technologies, on December 19, 2018 at a temperature of 21.8 °C and a relative humidity of 65%. The first step was to prepare molds. The inside of the moulds were cleaned from impurities from the previous casting and subsequently coated with Vaseline. This lubricant serves as an excellent separating agent, and forms an adherent layer between the casting and the mould, so that the cured casting can be easily removed from the mould. Then dosing was done. The dosing was carried out by measuring the volumes of the individual components using plastic and glass measuring cups.

*Figure 5. Measuring the volume of components*

The exact content of the components is shown in the following table.

*Table 3. Proportion of components in the test bodies*

| | |
|---|---|
| Test bodies no. 1,2 and 7 | |
| Filler 84% | 35% Danube gravel, 8 – 16 mm |
| | 35% Danube gravel, 4 – 8 mm |
| | 30% silica sand, 0,3 – 1 mm |
| Binder 16% | 100 parts LH 160 |
| | 50 parts H 287 |
| Test bodies no. 3,4 and 8 | |
| Filler 84% | 35% dolomic limestone, 8 – 16 mm |
| | 35% dolomic limestone, 4 – 8 mm |
| | 30% silica sand, 0,3 – 1 mm |
| Binder 16% | 100 parts LH 160 |
| | 50 parts H 287 |
| Test bodies no. 5,6 and 9 | |
| Filler 84% | 35% andesite, 8 – 16 mm |
| | 35% andesite, 4 – 8 mm |
| | 30% silica sand, 0,3 – 1 mm |
| Binder 16% | 100 parts LH 160 |
| | 50 parts H 287 |

The three filler fractions in each sample were mixed manually with each other for their addition to the binder, so that their distribution in the mixture was as homogeneous as possible. Subsequently, resin and hardener were mixed in another vessel using a Makita UT 1200 electric stirrer. It was stirred for 3 minutes. Active hydrogen ions with epoxy groups reacted and an exothermic reaction started. Subsequently, the filler was gradually added. The mixture was stirred for next 3 minutes until the resin were coated uniformly all of the filler.

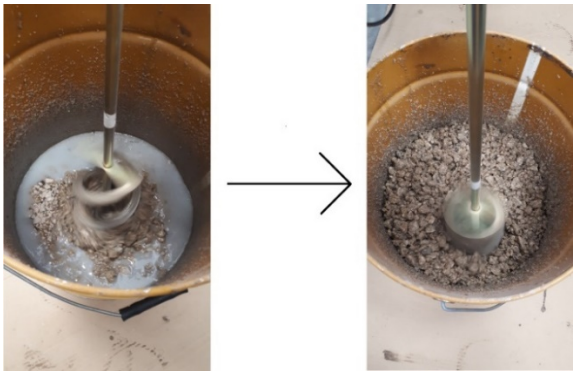

*Figure 6. Mixing the binder and the filler together*

After thorough mixing, the prepared form was filled. The Lievers LTT 40/40 was used after filling. It vibrated for about 2 minutes. During this process, air bubbles appeared on the surface. This reduces the porosity to a minimum. The binder appeared on the surface, which was glossy and smooth, meaning enough vibration.

*Figure 7. Filling the mold and vibration on Lievers LTT 40/40*

After vibrating, the filled mould was placed on a horizontal surface, and after 24 hours, castings were removed from the mould. The hardening of the castings took place for the next 15 days in the same room at 20-22 °C. After this time or more, the castings get the final properties and could be tested.

## 4. Testing the strength characteristics

Testing consisted of the following experiments: compression strength tests – test bodies in the shape of a cube, flexural strength tests – test bodies in the shape of joist.

*Figure 8. Test bodies*

First, we checked the dimensions according to standard STN EN 12390-1. This standard specifies the prescribed shapes and sizes of the test bodies, and possible errors of their dimensions. Dimensions were controlled by a calibrated digital sliding scale Mitutoyo ABSOLUTE AOS 500 series. Its accuracy is within ± 0.02 mm. All the test bodies passed through control.

*Figure 9. Dimension control*

The next step in the process is weighting of test bodies and determination of specific weight. This was done accordingly to standard STN EN 12390-7. This standard specifies the requirements for the used apparatus, and the procedure for determining of specific weight. The standard specifies three methods for determining the volume of the test bodies:

- by dipping into the water,
- by calculation from the measured dimensions,
- by calculation from selected measured dimensions (using calibrated forms).

In this case, the volume was determined by calculation from the measured dimensions, since dimension measurement was already performed at the dimension control in the previous step. After the volume was calculated, the test bodies were weighed.

Weighing was done on calibrated high-resolution digital scale Sartorius®-EA150-FEG-1. Its accuracy is within ± 5 g.

*Figure 10. Weighting of test bodies*

From the calculated volume, according to the measured dimensions and the measured weight, specific weight was calculated by following formula:

$$D = \frac{m}{V} \quad (1)$$

in which:

D is specific weight of test bodies [kg/m$^3$]
m is weight of test bodies [kg]
V is the volume of test bodies [m$^3$]
The following table shows the measured dimensions, weight, and determination of the specific weight.

*Table 4. Features of test bodies*

| Sample shape | Test body number | Dimensions | | | Weight [kg] | Specific weight [kg/m$^3$] |
|---|---|---|---|---|---|---|
| | | Push area [mm] | | Height [mm] | | |
| Cube | 1 | 149,6 | 150,2 | 150,1 | 7,060 | 2 090 |
| | 2 | 150,2 | 150,2 | 150,2 | 7,440 | 2 200 |
| | 3 | 149,8 | 149,8 | 150,1 | 7,545 | 2 230 |
| | 4 | 148,7 | 150,1 | 150,2 | 7,425 | 2 220 |
| | 5 | 150,9 | 150,1 | 150,1 | 7,255 | 2 140 |
| | 6 | 151,1 | 149,8 | 149,8 | 7,215 | 2 130 |
| Joist | | Width | Height | Length | | |
| | 7 | 99,7 | 100,2 | 499,9 | 11,085 | 2220 |
| | 8 | 99,5 | 100,1 | 500,4 | 11,035 | 2210 |
| | 9 | 100,7 | 100,1 | 499,8 | 10,820 | 2150 |

Then a measurement of the compressive strength according to standard STN EN 12390-3 was made. Considering the testing, force-measuring machine CONTROLS, model: 50-C0050 / HRD7 was used.

*Figure 11. Compressive strength test*

The force-measuring machine experienced the maximum pushing force. After that the compressive strength was calculated by the following formula:

$$\sigma_c = \frac{F}{A_C} \quad (2)$$

, in which:

$\sigma_c$ is compressive strength [MPa]
F is maximum compressive force [N]
$A_C$ is pressure area [mm$^2$]
The following table shows the maximum compressive force measured and the calculated compressive strength.

*Table 5. Compressive strength of test bodies*

| Test body number | Maximum compressive force [kN] | Compressive strength [MPa] | | |
|---|---|---|---|---|
| | | Calculated value | Round value ± U (k=2) | Average value |
| 1 | 1 262,4 | 56,22 | 56,2 ± 0,7 | 62,2 |
| 2 | 1 536,5 | 68,15 | 68,2 ± 0,8 | |
| 3 | 1 843,1 | 82,10 | 82,1 ± 0,9 | 80,0 |
| 4 | 1 737,9 | 77,92 | 77,9 ± 0,9 | |
| 5 | 1 957,3 | 86,45 | 86,5 ± 1,0 | 85,4 |
| 6 | 1 907,8 | 84,27 | 84,3 ± 1,0 | |

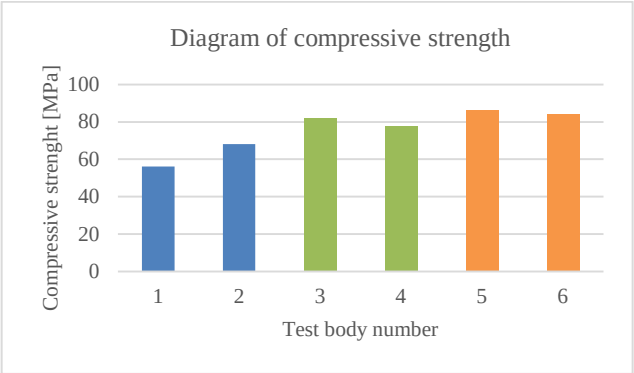


*Figure 12 . Graphical representation of compressive strength for various test bodies*

Figure 12 shows comparison of compressive strength for individual test bodies. As it can be observed from Figure 12, value of compressive strength of individual test bodies for same fillers is in similar range. The highest compressive strength was measured for test bodies number 5 and 6 with andesite as a filler. Good results were also obtained for test bodies number 3 and 4 with dolomic limestone as a filler. The smallest value of compressive strength was shown by test bodies number 1 and 2 with danube gravel as a filler.
Finally flexural strength test were made according to standard STN EN 12390-5. For testing, the force-

measuring machine CONTROLS, model: 50-C1201/* was used.

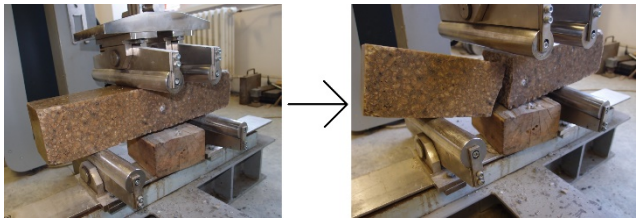

*Figure 13. Flexural strength test*

The force-measuring machine recorded the maximum load possible, and returned to its initial position. After that the flexural strength was calculated by following formula:

$$\sigma_{cf} = \frac{F \times l}{d_1 \times d_2^2} \quad (3)$$

, in which:
$\sigma_{cf}$ is flexural strength [MPa/s]
F is maximum load [N]
l is distance between supporting rollers [mm]
$d_1$, $d_2$ is cross-section dimensions [mm]

The table on next page shows the maximum load force measured and the calculated flexural strength.

*Table 6. Flexural strength of test bodies*

| Test body number | Maximum load force [kN] | Flexural strength [MPa] |
|---|---|---|
| | | Round value ± U (k=2) |
| 7 | 30,26 | 9,1 ± 0,3 |
| 8 | 36,31 | 10,9 ± 0,3 |
| 9 | 30,44 | 9,0 ± 0,3 |

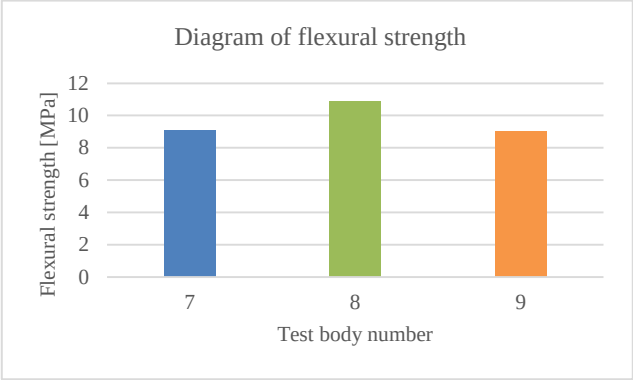


*Figure 14 Graphical representation of flexural strength for various test bodies*

Figure 12 shows comparison of flexural strength for the individual test bodies. As it can be observed from Figure 12 highest flexural strength was measured for test body number 8. The measured differences between the test bodies were relatively small. The influence of aggregate on flexural strength is negligible. The main factor influencing the flexural strength is mechanical parameters of the resin used. If necessary, in order to increase the flexural strength, different types of fibers can be used.

## 5. Conclusion

Polymer concrete castings can be tested in non-destructive and destructive ways. The destructive tests are protracted and more expensive than hardness test by Schmidt Hammer. They are more accurate and the results can be considered reliable. Destructive tests have proven, that from the three compared aggregates, polymer concrete castings with andesite have the highest compressive strength with average value 85,4 MPa. In second place were polymer concrete castings with dolomitic limestone whose average compressive strength was 80 MPa. The lowest compressive strength had polymer concrete castings with the Danube gravel as a filler. The flexural strength test proven, than the highest value of this parameter reached the test body number 8 containing dolomic limestone. The differences in the value of this parameter were approximately 2 MPa between the test bodies. Flexural strength will be increased by the use of fibers in the manufacture of next test bodies. The results of these tests will be published in the following publications.

**Acknowledgements**

*This work was supported by the Slovak Research and Development Agency under the contract No. APVV-15-0700 and paper is the result of the Project implementation: Competency Centre for Knowledge technologies applied in Innovation of Production Systems in Industry and Services, ITMS: 26220220155, supported by the Research & Development Operational Programme funded by the ERDF.*

**References**


[1]. Sadilek, M., Fojtík, F., Sadílková, Z., Kolařík, K., & Petrů, J. (2015). A study of effects of changing the position of the tool axis against the machined surface. *Transactions of FAMENA*, *39*(2), 33-46.

[2]. Orlovský, I., Hatala, M., & Duplák, J. (2014). Balance equation-an essential element of the definition of the drying process. In *Advanced Materials Research* (Vol. 849, pp. 310-315). Trans Tech Publications.

[3]. Trofimov, A., Mishurova, T., Lanzoni, L., Radi, E., Bruno, G., & Sevostianov, I. (2018). Microstructural analysis and mechanical properties of concrete reinforced with polymer short fibers. *International Journal of Engineering Science*, *133*, 210-218.

[4]. Jin, N. J., Yeon, J., Min, S. H., & Yeon, K. S. (2018). Strength Developments and Deformation Characteristics of MMA-Modified Vinyl Ester Polymer Concrete. *International Journal of Concrete Structures and Materials*, *12*(1), 4.

[5]. Şimşek, B., & Uygunoğlu, T. (2018). A full factorial-based desirability function approach to investigate optimal mixture ratio of polymer concrete. *Polymer Composites*, *39*(9), 3199-3211.

[6]. Li, L., Lu, J., Fang, S., Liu, F., & Li, S. (2017). Flexural study of concrete beams with basalt fibre polymer bars. *Proceedings of the Institution of Civil Engineers-Structures and Buildings*, *171*(7), 505-516.

[7]. Zegardło, B., Szeląg, M., Ogrodnik, P., & Bombik, A. (2018). Physico-mechanical properties and microstructure of polymer concrete with recycled glass aggregate. *Materials*, *11*(7), 1213.

[8]. Niaki, M. H., Fereidoon, A., & Ahangari, M. G. (2018). Effect of basalt, silica sand and fly ash on the mechanical properties of quaternary polymer concretes. *Bulletin of Materials Science*, *41*(3), 69.

[9]. Tanyildizi, H., & Asilturk, E. (2018). Performance of Phosphazene-Containing Polymer-Strengthened Concrete after Exposure to High Temperatures. *Journal of Materials in Civil Engineering*, *30*(12), 04018329.

[10]. Hu, B., Zhang, N., Liao, Y., Pan, Z., Liu, Y., Zhou, L., ... & Jiang, Z. (2018). Enhanced flexural performance of epoxy polymer concrete with short natural fibers. *Science China Technological Sciences*, *61*(8), 1107-1113.

[11]. Schmitt, A., Carvelli, V., Haffke, M. M., & Pahn, M. (2018). Thermo-mechanical response of concrete sandwich panels reinforced with glass fiber reinforced polymer bars. *Structural Concrete*, *19*(3), 839-850.

[12]. Burlacu, A., Ciocan, V., Şerbănoiu, A. A., Barbuţă, M., Verdeş, M., & Cojocaru, A. (2018). Study on Polymer Concretes With Waste of Polystyrene Granules. *Environmental Engineering & Management Journal (EEMJ)*, *17*(5), 1229-1235.

[13]. Niaki, M. H., Fereidoon, A., & Ahangari, M. G. (2018). Experimental study on the mechanical and thermal properties of basalt fiber and nanoclay reinforced polymer concrete. *Composite Structures*, *191*, 231-238.